Fault Tolerant Control of Magnetic Bearings with Force Invariance

Uhn Joo Na*

Division of Mechanical and Automation Engineering, Kyungnam University, Masan, Kyungnam 631-701, Korea

A magnetic bearing even with multiple coil failure can produce the same decoupled magnetic forces as those before failure if the remaining coil currents are properly redistributed. This fault-tolerant, force invariance control can be achieved with simply replacing the distribution matrix with the appropriate one shortly after coils fail, without modifying feedback control law. The distribution gain matrix that satisfies the necessary constraint conditions of decoupling linearized magnetic forces is determined with the Lagrange Multiplier optimization method.

Key Words : Magnetic Bearings, Fault Tolerance, Rotor Dynamics, Active Vibration Control

Nomenclature

a : Pole face area
b_{sat} : Saturation flux density
g_0 : Nominal air gap distance
q : Number of active poles
n : Number of coil turns
α : Path reluctance factor
σ : Leakage and fringing factor
λ : Lagrange multiplier
μ_0 : Permeability of air
μ_{rel} : Relative permeability
θ : Pole face angle

1. Introduction

A magnetic bearing system is a mechatronics device consisting of a magnetic force actuator (a magnetic bearing, or MB), motion sensors, power amplifiers, and a feedback controller (DSP), that is used to suspend the spinning rotor magnetically as well as to suppress vibrations actively. Magnetic bearings are filling a greater number of applications in industry since they have many advantages over conventional fluid film or rolling element bearings, such as lower friction losses, free of lubrication, operation at temperature extremes, quiet operation, and high speeds. Magnetic suspension produces active damping and stiffness which arises from the control action, so system parameters can be designed to avoid resonance or for optimum damping through the resonances while in operation. The design and control of magnetic bearings has been investigated by many researchers (Salm and Schweitzer, 1984, Matsumura and Yoshimoto, 1986, Jeon et al., 2002, Ahn and Han, 2003).

Highly critical applications of these machinery elements may demand a fault-tolerant control strategy. Fault-tolerant control of magnetic bearing system provides continued operation of the bearing even if its power amplifiers or coils suddenly fail. The goal of the present work is to develop a fault-tolerant control algorithm such that bearing actuators can preserve the same magnetic forces even after some components such as coils or power amplifiers fail. Fault-tolerant actuators were investigated by several researchers. Lyons et al. (1994) used a three control axis radial bearing structure with control algorithms for redundant force control and rotor position measurement. In this approach, if one of the coils fails, its entire control axis is shut down, while

* **E-mail** : uhnjoona@kyungnam.ac.kr
TEL : +82-55-249-2162; **FAX** : +82-55-249-2617
Division of Mechanical and Automation Engineering, Kyungnam University, Masan, Kyungnam 631-701, Korea. (Manuscript **Received** November 10, 2003; **Revised** June 23, 2004)

still maintaining control. Maslen and Meeker (1995) and Meeker (1996) showed that a magnetic bearing with multiple coil failure can produce decoupled control forces if the remaining coil currents are properly redistributed. The flux coupling between poles in a heteropolar magnetic bearing and reassigning of the remaining coil currents provides a mean to produce desired force resultants in the x and y directions when some coils fail. A fault tolerant magnetic bearing system was demonstrated by Maslen et al.(1999) on a large flexible-rotor test rig. Na and Palazzolo (2000) show that the fault-tolerant control can be maintained for an 8-pole magnetic bearing including material path reluctances for up to 5 coils out of 8 failed. The fault-tolerant scheme utilizing the grouping of currents reduces the required number of controller outputs and decoupling chokes (Na and Palazzolo, 2001). This fault tolerance may reduce load capacity of the bearing because the redistribution of currents to the failed bearing may lead to saturation in the bearing material.

The present work utilizes the bias voltage linearization to determine the redistribution of the remaining coil currents such that the same linearized magnetic forces are preserved even after the magnetic bearing actuator experiences failure. This represents an advance over previous methods (Maslen and Meeker, 1995; Na and Palazzolo, 2000) that provide x, y control force decoupling and linearized control force/control voltage relations, however do not preserve control force/control voltage gain and ignore position stiffness alteration with failure.

2. Bearing Model

Magnetic forces are determined from magnetic flux density and may be reduced by flux leakage, fringing, saturation of magnetic material, and eddy current effects. Flux density increases with magnetomotive force until it reaches a maximum point (saturation point), and further increase in currents will result in a very small increase in flux density. Maximum load of a magnetic bearing is thereby limited by material saturation. Eddy currents also reduce dynamic forces and can be reduced by properly laminating the journal and stator components. If eddy current effects are negligible, and the flux density is linear with magnetomotive force, Maxwell's equations can be fairly accurately approximated by 1D magnetostatic relations. An 8-pole heteropolar radial magnetic bearing is shown in Figure 1. The flux density in the air gap may be reduced due to the leakage and fringing effects which are accounted for by derating the force with a simple scaling factor (Allaire, 1989). The flux density vector in the air gap is described as;

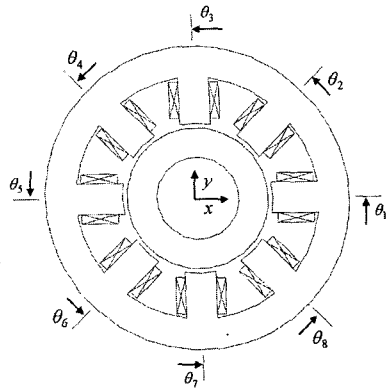

Fig. 1 Heteropolar Magnetic Bearing

$$B=V(x, y)I, \tag{1}$$

where the current vector is;

$$I=[i_1, i_2, \cdots, i_g]$$

A derivation of the current to flux density matrix appears in Appendix A. The magnetic forces along the φ direction are related to current inputs and rotor displacements as;

$$f_\varphi=-I^T Q_\varphi(x, y)I, \quad \varphi=x \text{ or } y. \tag{2}$$

where $$Q_\varphi(x, y)=V^T\frac{\partial D}{\partial \varphi}V$$

$$D=diag(g_j(x, y)a/(2\mu_0))$$

and where the air gap is described as;

$$g_j=g_0-x\cos\theta_j-y\sin\theta_j$$

The current inputs to each pole are generally expressed with a linear combination of a bias voltage v_b, and control voltages v_{cx} and v_{cy}. The

current vector of an 8-pole magnetic bearing is defined as ;

$$I=Tv \tag{3}$$

where the distribution matrix is $T=[T_b T_x T_y]$, and the voltage vector is $v=[v_b, v_{cx}, v_{cy}]^T$. The current distribution of a conventional C-core based, 8-pole magnetic bearing is realized by winding 4 coil pairs, one for each group of 2 poles (a coil pair is wound on two adjacent poles in series with the opposite polarity). A typical current distribution matrix of a load-on-pole, 8-pole magnetic bearing with independent currents is described as ;

$$\tilde{T}=\begin{bmatrix} 1 & \cos(0) & \sin(0) \\ -1 & -\cos\left(\frac{2\pi}{8}\right) & -\sin\left(\frac{2\pi}{8}\right) \\ 1 & \cos\left(\frac{4\pi}{8}\right) & \sin\left(\frac{4\pi}{8}\right) \\ -1 & -\cos\left(\frac{6\pi}{8}\right) & -\sin\left(\frac{6\pi}{8}\right) \\ 1 & \cos\left(\frac{8\pi}{8}\right) & \sin\left(\frac{8\pi}{8}\right) \\ -1 & -\cos\left(\frac{10\pi}{8}\right) & -\sin\left(\frac{10\pi}{8}\right) \\ 1 & \cos\left(\frac{12\pi}{8}\right) & \sin\left(\frac{12\pi}{8}\right) \\ -1 & -\cos\left(\frac{14\pi}{8}\right) & -\sin\left(\frac{14\pi}{8}\right) \end{bmatrix} \tag{4}$$

where the first column, the second column, and the third column represent the bias vector, x control vector, and y control vector, respectively. Note that the currents are distributed to each pole by imposing a bias voltage and changing control voltages. With the uniform current distribution shown in Eq. (4) as well as the symmetric bearing geometries, magnetic forces are (x, y) decoupled and vary linearly with respect to control currents and rotor displacements around the bearing center position (Bornstein, 1991 ; Lee and Kim, 1992).

If some coils fail, the full (8×1) current vector is related to the reduced current vector by introducing a failure map matrix H.

$$I=H\hat{I}, \tag{5}$$

For example, if the 4-5-7th coils fail, the current vector is described as ;

$$I=\begin{bmatrix} i_1 \\ i_2 \\ i_3 \\ 0 \\ 0 \\ i_6 \\ 0 \\ i_8 \end{bmatrix}=\begin{bmatrix} 1 & 0 & 0 & 0 & 0 \\ 0 & 1 & 0 & 0 & 0 \\ 0 & 0 & 1 & 0 & 0 \\ 0 & 0 & 0 & 0 & 0 \\ 0 & 0 & 0 & 0 & 0 \\ 0 & 0 & 0 & 1 & 0 \\ 0 & 0 & 0 & 0 & 0 \\ 0 & 0 & 0 & 0 & 1 \end{bmatrix}\begin{bmatrix} \hat{i}_1 \\ \hat{i}_2 \\ \hat{i}_3 \\ \hat{i}_4 \\ \hat{i}_5 \end{bmatrix}=H\hat{I}$$

If symmetry is lost due to coil failure, magnetic forces are no longer decoupled and linear with respect to control currents and rotor displacements. If one or more of the 8 coils with the distribution matrix $\tilde{T}$ fail, the magnetic forces will be coupled and asymmetric. It may be difficult to maintain control if severe asymmetry is present due to multiple coil failures. Reassigning the remaining currents with a redifined current distribution scheme utilizing the flux coupling property of a heteropolar magnetic bearing may remedy this by providing the same decoupled magnetic forces as before failure. The reduced current vector is expressed as ;

$$\hat{I}=\hat{T}v \tag{6}$$

where the reduced distribution matrix is defined as ;

$$\hat{T}=[\hat{T}_b \hat{T}_x \hat{T}_y], \tag{7}$$

where

$$\hat{T}_b=[t_1, t_2, ..., t_q]^T,$$

$$\hat{T}_x=[t_{q+1}, t_{q+2}, ..., t_{2q}]^T,$$

$$\hat{T}_y=[t_{2q+1}, t_{2q+2}, ..., t_{3q}]^T$$

The optimal $\hat{T}$ should be determined in a manner such that the magnetic forces remain invariant before and after failure. The Lagrange Multiplier optimization with equality constraints is used to determined the optimal $\hat{T}$. The remaining currents redistributed by the optimal $T=H\hat{T}$ provide the same magnetic forces before and after failure, which means that the dynamics of the rotor is not disturbed by coil failure. The distribution matrix T can be implemented in DSP

controller as a part of a control law so that the effects of a coil failure can be very much mitigated with control action. The magnetic forces are controlled with a combination of 8 currents one for each pole in normal operation. However, the minimum number of independent currents required for generating arbitrary magnetic forces is three (Meeker, 1996). This describes the basic fault tolerance action, i.e. if some coils fail, the remaining coils must provide the magnetomotive forces to generate the desired magnetic forces.

3. Linearization of Magnetic Forces

The general magnetic forces including a distribution gain matrix and the control voltage vector are described as ;

$$f_\varphi = v^T M_\varphi v \tag{8}$$

where

$$M_\varphi = -\hat{T}^T H^T Q_\varphi(x, y) H \hat{T} \tag{9}$$

The magnetic forces are quadratically dependent on the voltage vector v. The bias voltage v_b is adjusted in a manner that maximizes the load capacity of the magnetic bearing. The magnetic forces in Eq. (8) are linearized about the bearing center position and about the bias voltage v_b (Na and Palazzolo, 2000). The linearized magnetic forces are then ;

$$\begin{bmatrix} f_x \\ f_y \end{bmatrix} = -\begin{bmatrix} k_{pxx} & k_{pxy} \\ k_{pyx} & k_{pyy} \end{bmatrix}\begin{bmatrix} x \\ y \end{bmatrix} + \begin{bmatrix} k_{vxx} & k_{vxy} \\ k_{vyx} & k_{vyy} \end{bmatrix}\begin{bmatrix} v_{cx} \\ v_{cy} \end{bmatrix} \tag{10}$$

or

$$F = -K_p z + K_v v_c \tag{11}$$

The position related force coefficients (position stiffnesses) are calculated as

$$k_{p\varphi\omega} = -\frac{\partial f_\varphi}{\partial \omega} = -T_b^T Q_{\varphi\omega 0} T_b v_b^2, \tag{12}$$

where

$$Q_{\varphi\omega 0} = \frac{\partial Q_\varphi}{\partial \omega}\bigg|_{\substack{\varphi=0 \\ \omega=0}} = 2V \frac{\partial D}{\partial \varphi}\frac{\partial V^T}{\partial \omega}\bigg|_{\substack{\varphi=0 \\ \omega=0}} \tag{13}$$

and the voltage related force coefficients (voltage stiffnesses) are ;

$$k_{v\varphi\omega} = \frac{\partial f_\varphi}{\partial v_{c\omega}} = -2 T_b^T Q_{\varphi 0} T_\omega v_b, \tag{14}$$

where

$$Q_{\varphi 0} = Q_\varphi|_{\substack{\varphi=0 \\ \omega=0}}$$

where the parameters φ and ω both represent x or y direction. For example, the linearized magnetic forces with the distribution matrix $\tilde{T}$ for an unfailed bearing are ;

$$f_\varphi = -k_p \varphi + k_v v_{c\varphi} \tag{15}$$

where

$$k_p = -\tilde{T}_b^T Q_{\varphi\omega 0} \tilde{T}_b v_b^2, \tag{16}$$

$$k_v = -2 \tilde{T}_b^T Q_{\varphi 0} \tilde{T}_\varphi v_b, \tag{17}$$

The linearized magnetic forces for an unfailed bearing are completely decoupled as shown in Eq. (15). However, if some coils in the bearing fail with the current distribution scheme of $\tilde{T}$, the linearized forces in Eq. (10) may become full matrices, and may be strongly asymmetric.

4. Fault Tolerance of Magnetic Forces

4.1 Decoupling of control dependent magnetic forces

Employing an optimal current distribution T may decouple the linearized forces, and even maintain the same decoupled magnetic forces as those of an unfailed magnetic bearing. Maslen and Meeker (1995) introduced a linearization method which effectively decouple the control forces for a failed bearing by choosing a proper distribution matrix. Though not identified in (Maslen and Meeker, 1995), the necessary conditions to yield the same decoupled control forces as those of the unfailed bearing are ;

$$\hat{M}_x = \frac{k_v}{v_b}\begin{bmatrix} 0 & \frac{1}{2} & 0 \\ \frac{1}{2} & 0 & 0 \\ 0 & 0 & 0 \end{bmatrix}, \quad \hat{M}_y = \frac{k_v}{v_b}\begin{bmatrix} 0 & 0 & \frac{1}{2} \\ 0 & 0 & 0 \\ \frac{1}{2} & 0 & 0 \end{bmatrix} \tag{18}$$

If M_φ in Eq. (9) are determined such that Eq. (18) should be satisfied, the off-diagonal voltage terms in Eq. (8) can then be effectively eliminated. The magnetic forces f_φ at the bearing center

position then become;

$$f_\varphi = k_v v_{c\varphi} \tag{19}$$

Substituting $\tilde{T}$ in Eq. (9) for the normal operation leads to Eq. (18). If the distribution matrix T is determined in case of a coil failure such that M_φ should be invariant as Eq. (18) through coil failures, the magnetic forces are then only dependent on the control voltage vector. If M_φ in Eq. (9) is equal to the condition in Eq. (18), the magnetic forces can be linearized to Eq. (19) even in case of coil failure. Eq. (9) and Eq. (18) can be written in 18 scalar forms, and then boils down to 12 algebraic equations if redundant terms are eliminated. The equality constraints to yield the same control forces before and after failure are;

$$\begin{aligned}
h_1(\hat{T}) &= \hat{T}_b{}^T H^T Q_{x0} H \hat{T}_b = 0 \\
h_2(\hat{T}) &= \hat{T}_b{}^T H^T Q_{y0} H \hat{T}_b = 0 \\
h_3(\hat{T}) &= \hat{T}_b{}^T H^T Q_{x0} H \hat{T}_y = 0 \\
h_4(\hat{T}) &= \hat{T}_b{}^T H^T Q_{y0} H \hat{T}_x = 0 \\
h_5(\hat{T}) &= \hat{T}_x{}^T H^T Q_{x0} H \hat{T}_x = 0 \\
h_6(\hat{T}) &= \hat{T}_y{}^T H^T Q_{x0} H \hat{T}_y = 0 \\
h_7(\hat{T}) &= \hat{T}_x{}^T H^T Q_{y0} H \hat{T}_x = 0 \\
h_8(\hat{T}) &= \hat{T}_y{}^T H^T Q_{y0} H \hat{T}_y = 0 \\
h_9(\hat{T}) &= \hat{T}_y{}^T H^T Q_{x0} H \hat{T}x = 0 \\
h_{10}(\hat{T}) &= \hat{T}_x{}^T H^T Q_{y0} H \hat{T}_y = 0 \\
h_{11}(\hat{T}) &= \hat{T}_b{}^T H^T Q_{x0} H \hat{T}_x - \frac{k_v}{2v_b} = 0 \\
h_{12}(\hat{T}) &= \hat{T}_b{}^T H^T Q_{y0} H \hat{T}_y - \frac{k_v}{2v_b} = 0
\end{aligned} \tag{20}$$

4.2 Decoupling of position dependent magnetic forces

The conditions for decoupling control voltage related forces are necessary for the fault-tolerant control but may not be sufficient since position dependent forces may still become (x, y) coupled and asymmetric, potentially leading to performance and stability degradation. Asymmetric closed loop stiffnesses may create elliptic orbits or force orbits offcenter. Some cross coupled position stiffnesses also act like negative dampings, and may reduce the stability margin of the closed loop system. The position related forces in Eq. (11) can be decoupled if the distribution matrix is adjusted in a manner that the cross-coupled position stiffness terms should be equal to zero. The conditions for eliminating the off-diagonal cross coupled position stiffnesses are;

$$\begin{aligned}
h_{13}(\hat{T}) &= \hat{T}_b{}^T H^T Q_{xy0} H \hat{T}_b = 0 \\
h_{14}(\hat{T}) &= \hat{T}_b{}^T H^T Q_{yx0} H \hat{T}_b = 0
\end{aligned} \tag{21}$$

The conditions for the direct position stiffnesses to have the same values as those of an unfailed bearing are;

$$\begin{aligned}
h_{15}(\hat{T}) &= \hat{T}_b{}^T H^T Q_{xx0} H \hat{T}_b - \frac{k_p}{v_b{}^2} = 0 \\
h_{16}(\hat{T}) &= \hat{T}_b{}^T H^T Q_{yy0} H \hat{T}_b - \frac{k_p}{v_b{}^2} = 0
\end{aligned} \tag{22}$$

It is notable that the position dependent forces are only influenced by the bias components of the distribution matrix. If there exists a distribution matrix that satisfies the conditions described in Eqs. (20)-(22), the same linearized magnetic forces will be generated before and after failure. Previous approaches to the fault tolerance problem did not address position stiffness changes and asymmetry, nor voltage stiffness value changes after failure (Maslen and Meeker, 1995, Meeker, 1996).

5. Optimization

There may exist multiple candidates of $\hat{T}$'s that satisfy the decoupling conditions. The criterion for choosing the best candidate is the one that will yield the maximum load capacity prior to any saturation. To accomplish this a distribution matrix $\hat{T}$ can be determined by using the Lagrange Multiplier method to minimize the Euclidean norm of the flux density vector B (Na and Palazzolo, 2000). The cost function is defined as;

$$J = B(\hat{T})^T P B(\hat{T}) \tag{23}$$

where the diagonal weighting matrix P is also selected to maximize the load capacity.

The Lagrange Multiplier method is then used to solve for the T that satisfies Eq. (23). Define:

$$L(\hat{T})=B(\hat{T})^{T}PB(\hat{T})+\sum_{j=1}^{16}\lambda_j h_j(\hat{T}) \quad (24)$$

Partial differentiation of Eq. (25) with respect to t_i and λ_j leads to $3q+16$ nonlinear algebraic equations to solve for t_i and λ_j.

$$W=\begin{bmatrix} w_1(t,\lambda) \\ w_2(t,\lambda) \\ \vdots \\ w_{3q+15}(t,\lambda) \\ w_{3q+16}(t,\lambda) \end{bmatrix}=0, \quad (25)$$

where

$$w_i=\frac{\partial L}{\partial t_i}=0,\ i=1,2,...,3q$$

$$w_{(j+3q)}=h_j(\hat{T})=0,\ i=1,2,...,16$$

The system of nonlinear algebraic equations shown in Eqs. (25) can be solved for the distribution matrix $\hat{T}(t_i)$ (Na and Palazzolo, 2000). A least square iterative method was used to solve the system of nonlinear algebraic equations, which yields multiple solutions (local optima). Various initial guesses were tested until they converged to the solution within tolerable errors. The 8-pole heteropolar magnetic bearing used in this analysis has g_0(0.0005m), (0.0005236m^2), n(60). The calculated distribution matrix for the 7-8th coils failed bearing is;

$$T_{78}=\begin{bmatrix} 1.9972 & 1.4996 & -0.6189 \\ 2.0066 & 1.2148 & -0.4977 \\ 0.0094 & 0.7144 & -1.9482 \\ -0.0093 & 0.7144 & -1.9482 \\ 1.9934 & -0.7852 & -1.3294 \\ 2.0027 & -0.5004 & -1.4505 \\ 0 & 0 & 0 \\ 0 & 0 & 0 \end{bmatrix} \quad (26)$$

Equation (18) is satisfied with the calculated T_{78} as shown in

$$M_x=\begin{bmatrix} 0 & 19.3985 & 0 \\ 19.3985 & 0 & 0 \\ 0 & 0 & 0 \end{bmatrix},\ M_y=\begin{bmatrix} 0 & 0 & 19.3985 \\ 0 & 0 & 0 \\ 19.3985 & 0 & 0 \end{bmatrix}$$

and the calculated distribution matrix for the 6-7-8th coils failed bearing is;

$$T_{678}=\begin{bmatrix} 2.3295 & 1.8011 & -1.7642 \\ 0.9996 & -0.0024 & -3.9096 \\ 3.0955 & 0 & -2.7502 \\ 0.9996 & 0.0024 & -3.9096 \\ 2.3295 & -1.8011 & -1.7642 \\ 0 & 0 & 0 \\ 0 & 0 & 0 \\ 0 & 0 & 0 \end{bmatrix} \quad (27)$$

Equation (18) is satisfied with the calculated T_{678} as shown in

$$M_x=\begin{bmatrix} 0 & 19.3985 & 0 \\ 19.3985 & 0 & 0 \\ 0 & 0 & 0 \end{bmatrix},\ M_y=\begin{bmatrix} 0 & 0 & 19.3985 \\ 0 & 0 & 0 \\ 19.3985 & 0 & 0 \end{bmatrix}$$

and the 2-4-7-8th coils failed bearing is;

$$T_{2478}=\begin{bmatrix} 2.0349 & 4.2171 & -1.3317 \\ 0 & 0 & 0 \\ 1.9361 & 0.0221 & 1.7773 \\ 0 & 0 & 0 \\ -0.6927 & -4.2573 & 2.3976 \\ -1.7853 & -0.1133 & 1.8531 \\ 0 & 0 & 0 \\ 0 & 0 & 0 \end{bmatrix} \quad (28)$$

Equation (18) is satisfied with the calculated T_{2478} as shown in

$$M_x=\begin{bmatrix} -0.3983 & 19.1959 & -0.5401 \\ 19.1959 & -0.3316 & -1.7689 \\ -0.54301 & -1.7689 & -2.3590 \end{bmatrix}$$

$$M_y=\begin{bmatrix} 1.4598 & -0.3243 & 18.5044 \\ -0.3243 & -0.0254 & 0.6567 \\ 18.5044 & 0.6567 & 0.8839 \end{bmatrix}$$

It is interesting to note that the linearized forces in Eqs. (10) and (11) result in the same position and voltage stiffnesses when any of the distribution matrices for different failure cases in Eqs. (26)-(27) is used. However, the distribution matrix for the 4 coils failed case such as Eq. (28) has off-diagonal error terms in M_φ. It may be difficult to find the exact solution for the hard failure such as 4 or more coils failed bearings because of the geometric limitation. However, the optimization algorithm try to find the approximate solution that nearly satisfy the 16 constraints with some error residuals remained.

Table 1 The calculated linearized forces

	$\tilde{T}$	$\breve{T}_{78}$	T_{78}	$\breve{T}_{678}$	T_{678}	$\breve{T}_{2478}$	T_{2478}
k_{pxx}(N/m)	912880	929030	912860	946470	912930	681510	919840
k_{pxy}(N/m)	0	36795	-6.2	-5772	0	141500	72692
k_{pyx}(N/m)	0	36795	-6.2	-5772	0	141500	72692
k_{pyy}(N/m)	912880	398600	912860	192280	912900	931810	835960
k_{vxx}(N/volt)	133.07	133.07	133.07	133.07	133.08	132.95	131.688
k_{vxy}(N/volt)	0	0	0	0	0	-0.23	-3.7
k_{vyx}(N/volt)	0	0	0	0	0	-0.03	-2.2
k_{vyy}(N/volt)	133.07	133.07	133.07	133.07	133.08	132.54	126.94

The main difference of the fault tolerant approach presented in this paper over the previous approaches is that the position stiffness constraints in Eqs. (21) and (22) are added in this paper. If there exist solutions for any failed bearing, the same position and voltage stiffnesses as those of the unfailed bearing can be maintained. Notable is the fact that these results are achieved without modifying the feedback control law after failure, nor requiring any type of control law. This clearly is a distinct advantage over previous other fault tolerant approaches. Previous fault tolerant approaches utilize only control force constraints in Eq. (20). Distribution matrices are calculated using only control force constraints in Eq. (20). The calculated distribution matrix for the 7-8th coils failed bearing is;

$$\breve{T}_{78}=\begin{bmatrix} 1.8703 & 1.6025 & -2.0254 \\ -0.2767 & -0.2371 & -2.9881 \\ 0.6040 & 0.5175 & -1.9344 \\ 1.7978 & -0.6612 & -0.1415 \\ 0.8807 & 0.7545 & -2.7072 \\ -0.7717 & 1.5404 & -0.1415 \\ 0 & 0 & 0 \\ 0 & 0 & 0 \end{bmatrix} \tag{29}$$

and the calculated distribution matrix for the 6-7-8th coils failed bearing is;

$$\breve{T}_{678}=\begin{bmatrix} 1.8316 & 1.4716 & -1.7612 \\ 0.0427 & 0.0387 & -3.87 \\ -0.0182 & 0.0012 & -3.2988 \\ -0.0143 & -0.0358 & -3.8715 \\ 1.8187 & -1.4702 & -1.8214 \\ 0 & 0 & 0 \\ 0 & 0 & 0 \\ 0 & 0 & 0 \end{bmatrix} \tag{30}$$

and the calculated distribution matrix for the 2-4-7-8th coils failed bearing is;

$$\breve{T}_{2478}=\begin{bmatrix} 1.7936 & 3.6522 & -1.7268 \\ 0 & 0 & 0 \\ 2.0471 & 1.4531 & 1.1691 \\ 0 & 0 & 0 \\ 0.4934 & 3.9197 & -1.4199 \\ 2.1833 & 1.1875 & -2.3468 \\ 0 & 0 & 0 \\ 0 & 0 & 0 \end{bmatrix} \tag{31}$$

The position stiffnesses in Eq. (12) and the voltage stiffnesses in Eq. (14) are evaluated for the distribution matrices of $\tilde{T}$, T_{78}, T_{678}, T_{2478}, $\breve{T}_{78}$, $\breve{T}_{678}$, $\breve{T}_{2478}$, and v_b of 3.43, and are shown in Table 1. Table 1 shows that the position stiffnesses as well as the voltage stiffnesses using T_{78}, T_{678}, T_{2478} for failed bearing are almost the same as those using $\tilde{T}$ for the unfailed bearing. The voltage stiffnesses using $\breve{T}_{78}$, $\breve{T}_{678}$, $\breve{T}_{2478}$ are the same as those of the unfailed bearing while the position stiffnesses using $\breve{T}_{78}$, $\breve{T}_{678}$, $\breve{T}_{2478}$ are different from those of the unfailed bearing, since no constraints are used for the position stiffnesses.

The 3-D finite element model is constructed for a heteropolar magnetic bearing by using a commercial magnetic field software (OPERA3D). The designed bearing properties are (0.0005 m), (0.0005236 m^2), and $n(60)$. Two current sets, $I_1=\tilde{T}v$ and $I_2=T_{2478}v$, with $v=[3.43\ \ 2\cos(\Omega t)\ \ 2\sin(\Omega t)]^T$ and $t=\pi/(6\Omega)$, are applied on the 3-D finite element model such that magnetic bearing flux distribution and the corresponding magnetic forces for the normal operation with $\tilde{T}$ should be compared with those of the fault to-

lerant operation with T_{2478}. Flux distribution in the bearing stator driven by I_1 and I_2 are shown in Fig. 2. It is notable that fluxes still flow through the failed poles (2^{nd}, 4^{th}, 7^{th}, and 8^{th} poles) due to flux coupling when I_2 is applied. This flux coupling in the failed bearing and optimal current distribution make possible to generate the same net magnetic forces as those of the unfailed bearing. The magnetic forces driven with I_1 and I_2 are also calculated using OPERA3D. The calculated magnetic forces shown in Table 2 indicate that the optimally distributed currents for the 2-4-7-8^{th} coils failed bearing produce very much the same magnetic forces as those of the unfailed bearing.

Table 2 Magnetic Forces Calculated with I_1 and I_2

	I_1	I_2
f_x(N)	295.12	305.18
f_y(N)	166.94	184.22

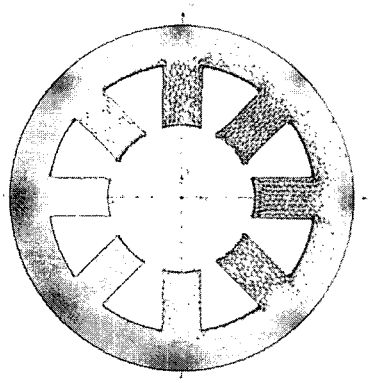

(a) Flux Distribution with I_1 (Normal Operation)

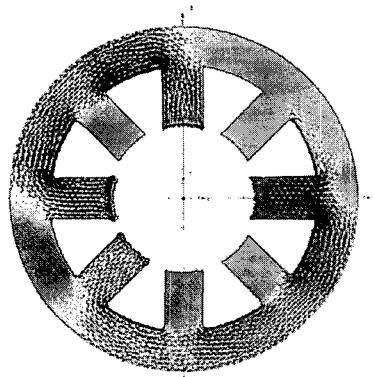

(b) Flux Distribution with I_2 (Fault Tolerant Operation)

Fig. 2 Fault Tolerant Flux Operation

6. Control System Design and Simulations

The feedback voltage control law can be designed excluding all fault tolerance considerations since the actuator's force-voltage and force-displacement characteristics are unaltered by the failure. A feedback control law used to stabilize the system is defined as ;

$$v_c = g(z, \dot{z}) \tag{32}$$

Note that any of the array of control algorithms (linear or nonlinear) for magnetic bearing systems appearing in the literature can be utilized with the fault tolerant scheme. The total current vector for the fault-tolerant magnetic bearing actuator is ;

$$I = I_b + I_c \tag{33}$$

where the redefined bias current is ;

$$I_b = T_b v_b, \tag{34}$$

and the redefined control current vector is ;

$$I_c = [T_x T_y] v_c = T_c v_c \tag{35}$$

For sake of illustration in this example, the closed loop bearing stiffness and damping may be adjusted by tuning the PD control gains (Keith, 1990). The fault-tolerant control scheme with the PD control law is illustrated in Fig. 3. The schematic of the rotor-bearing system is shown in Fig. 4. The T's can be calculated and stored in the database for all possible combinations of failure. Coil or power amplifier failure can be detected with the current sensors installed on all coils. If the failure status vector is determined

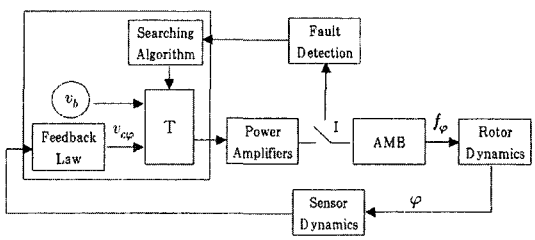

Fig. 3 Fault Tolerant Control Scheme

failure. Coil or power amplifier failure can be detected with the current sensors installed on all coils. If the failure status vector is determined from measurements, the corresponding T will be searched from the data base and replace the existing T.

The following system dynamics simulation illustrates the transient response of a rotor supported by magnetic bearings during a coil failure event. The horizontal, rigid rotor model has a mass of 12kg, Polar moment of inertia of 0.05 kg m^2, transverse moment of inertia of 0.36 kg m^2, and bearing locations of 0.22 m on each side of the mass center. Unbalances of eccentricity 1.0e-5 m are applied on two bearing locations with a relative phase angle of 90°. The rotor speed is held constant at 10,000 RPM. It is notable that although the algorithm presented preserves the linearized forces before and after coil failure, the simulation model employs nonlinear bearing forces as a more stringent test. PD control gains of K_p and K_d are designed to be 15 and 0.05 respectively. Displacement sensor and power amplifier gains are 7874 Volt/m and 1 Ampere/volt respectively. Figure 5 shows transient response displacement plots at Bearing A from the normal unfailed operation through coil failures (the 7-8^{th} coils failed at 0.1 sec., and the 6-7-8^{th} coils failed at 0.2 sec., and the 2-4-7-8^{th} coils failed at 0.3

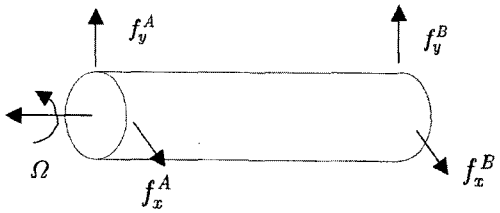

Fig. 4 Schematic of Rotor-Bearing System

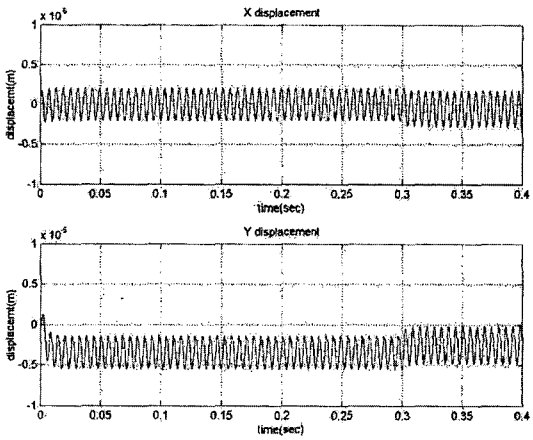

Fig. 5 The displacements at Bearing A (the 7-8^{th} coils failed at 0.1sec, and the 6-7-8^{th} coils failed at 0.2 sec)

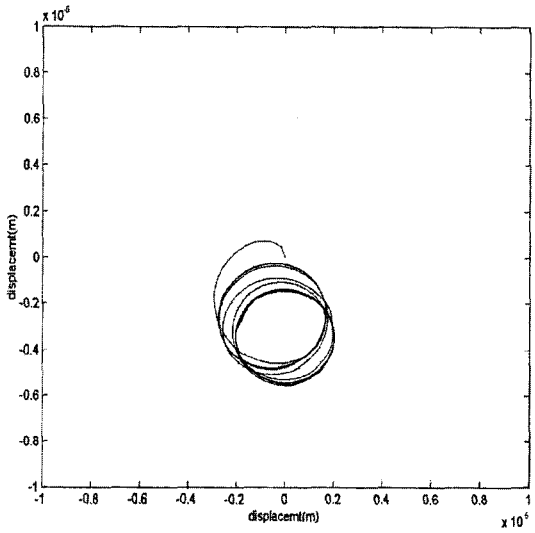

Fig. 6 The Orbits at Bearing A (the 7-8^{th} coils failed at 0.1sec, and the 6-7-8^{th} coils failed at 0.2sec)

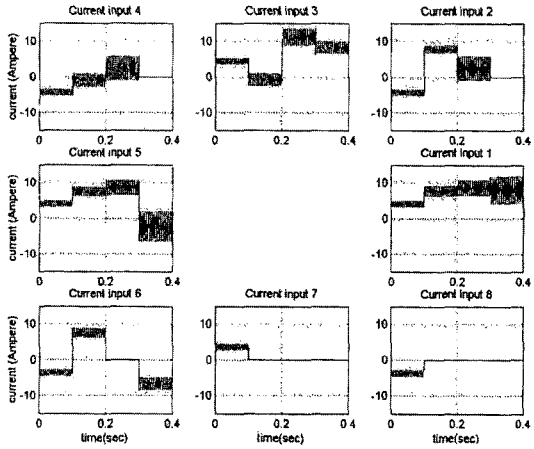

Fig. 7 Currents Through Bearing A (the 7-8^{th} coils failed at 0.1sec, and the 6-7-8^{th} coils failed at 0.2 sec)

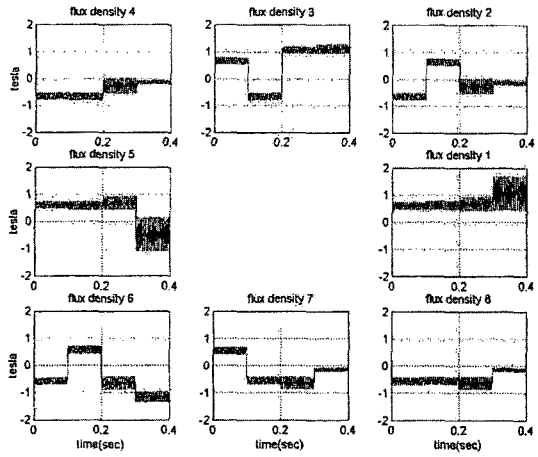

Fig. 8 Flux Densities at Bearing A (the 7-8th coils failed at 0.1sec, and the 6-7-8th coils failed at 0.2 sec)

sec.). An orbit plot at Bearing A through the failure sequence is shown in Figure 6. Transient response of the current inputs to bearing A is shown in Figure 7 and transient response of the flux densities in Bearing A is shown in Figure 8. Orbits are slightly disturbed after the 2-4-7-8th coils fail at 0.3 seconds, since the asymmetric and coupled position stiffnesses caused by T_{2478} do not provide the same closed loop dynamics as those of the unfailed bearing.

7. Conclusions

A current distribution gain matrix, T is determined so that the magnetic bearing actuator will preserve the same total linearized magnetic forces even after some components such as coils or power amplifiers experience failure. The present fault tolerant method provides complete decoupling of control dependent forces (voltage stiffnesses) as well as position dependent forces (position stiffnesses). This is a clear advance over previous methods. Fault tolerant simulations show that orbits after failure can be maintained very close to the orbit before failure even if the control gains are left unchanged after failure. Relatively large increase in currents and flux densities may be required to maintain the same closed loop dynamic properties after failure, depending on the nature of the disturbances. Therefore, disturbance levels from imbalance, runout or sideloads should be maintained at low levels to prevent saturation.

Acknowledgenents

This work was supported by Kyungnam university research fund.

Appendix A

Ampere's loop law, Gauss's law, and conservation of fluxes in the magnetic circuit provides the flux-current relation.

$$R\Phi=NI \tag{A1}$$

The flux density vector for the air gaps is ;

$$B=V(x, y)I, \tag{A2}$$

where

$$V=\frac{\sigma\mu_0 n}{g_0}\hat{R}^{-1}\hat{N} \tag{A3}$$

Reluctances in the magnetic bearing can be partitioned into a gap reluctance matrix and a material path reluctance matrix.

$$\hat{R}=\Re_g+\Re_m \tag{A4}$$

The non-dimensional gap reluctance matrix is ;

$$\Re_g=\begin{bmatrix} \hat{g}_1 & -\hat{g}_2 & 0 & 0 & 0 & 0 & 0 & \hat{g}_1 \\ 0 & \hat{g}_2 & -\hat{g}_3 & 0 & 0 & 0 & 0 & 0 \\ 0 & 0 & \hat{g}_3 & -\hat{g}_4 & 0 & 0 & 0 & 0 \\ 0 & 0 & 0 & \hat{g}_4 & -\hat{g}_5 & 0 & 0 & 0 \\ 0 & 0 & 0 & 0 & \hat{g}_5 & -\hat{g}_6 & 0 & 0 \\ 0 & 0 & 0 & 0 & 0 & \hat{g}_6 & -\hat{g}_7 & 0 \\ 0 & 0 & 0 & 0 & 0 & 0 & \hat{g}_7 & \hat{g}_8 \\ 1 & 1 & 1 & 1 & 1 & 1 & 1 & 1 \end{bmatrix} \tag{A5}$$

where the non-dimensional air gap equations are ;

$$\hat{g}_j=1-\hat{x}\cos\theta_j-\hat{y}\cos\theta_j \tag{A6}$$

where

$$\hat{x}=x/g_0 \text{ and } \hat{y}=y/g_0$$

The non-dimensional material path reluctance matrix is defined as ;

$$\mathfrak{R}_m=\frac{k}{\mu_{rel}}=\begin{bmatrix} 1+\frac{\eta}{8} & -1-\frac{6\eta}{8} & -\frac{5\eta}{8} & -\frac{4\eta}{8} & -\frac{3\eta}{8} & -\frac{2\eta}{8} & -\frac{\eta}{8} & 0 \\ \frac{\eta}{8} & 1+\frac{2\eta}{8} & -1-\frac{5\eta}{8} & -\frac{4\eta}{8} & -\frac{3\eta}{8} & -\frac{2\eta}{8} & -\frac{\eta}{8} & 0 \\ \frac{\eta}{8} & \frac{2\eta}{8} & 1+\frac{3\eta}{8} & -1-\frac{4\eta}{8} & -\frac{3\eta}{8} & -\frac{2\eta}{8} & -\frac{\eta}{8} & 0 \\ \frac{\eta}{8} & \frac{2\eta}{8} & \frac{3\eta}{8} & 1+\frac{4\eta}{8} & -1-\frac{3\eta}{8} & -\frac{2\eta}{8} & -\frac{\eta}{8} & 0 \\ \frac{\eta}{8} & \frac{2\eta}{8} & \frac{3\eta}{8} & \frac{4\eta}{8} & 1+\frac{5\eta}{8} & -1--\frac{2\eta}{8} & -\frac{\eta}{8} & 0 \\ \frac{\eta}{8} & \frac{2\eta}{8} & \frac{3\eta}{8} & \frac{4\eta}{8} & \frac{5\eta}{8} & 1+\frac{6\eta}{8} & -1-\frac{\eta}{8} & 0 \\ \frac{\eta}{8} & \frac{2\eta}{8} & \frac{3\eta}{8} & \frac{4\eta}{8} & \frac{5\eta}{8} & \frac{6\eta}{8} & 1+\frac{7\eta}{8} & -1 \\ 0 & 0 & 0 & 0 & 0 & 0 & 0 & 0 \end{bmatrix} \quad \text{(A7)}$$

$$\eta=\frac{\rho_J k_B+\rho_B k_J}{\rho_B \sigma_J}, \quad \text{(A8)}$$

where the areas of the poles, the back iron, and the journal iron are expressed in terms of the pole face area as $A_P=A$, $A_B=\rho_B A$, and $A_J=\rho_J A$. The length of the pole legs and the length of the back iron and of the journal between the two poles is given in terms of the nominal gap distance as $l_P=kg_0$, $l_B=kk_B g_0$, $l_J=kk_J g_0$. The coil turn matrix is;

$$\hat{N}=\begin{bmatrix} 1 & -1 & 0 & . & . & 0 \\ 0 & 1 & -1 & 0 & . & . \\ 0 & 0 & 1 & -1 & 0 & . \\ . & . & . & . & . & 0 \\ 0 & 0 & . & 0 & 1 & -1 \\ 0 & 0 & . & . & 0 & 0 \end{bmatrix} \quad \text{(A9)}$$

References

Ahn, H. and Han, D., 2003, "System Modeling and Robust Control of an AMB Spindle Part II A Robust Controller Design and its Implementation," *KSME International Journal*, Vol. 17 No. 12, pp. 1855~1866.

Allaire, P. E., 1989, "Design and Test of a Magnetic Thrust Bearing," *Journal of the Franklin Institute*, Vol. 326, No. 6, pp. 831~847.

Bornstein, K. R., 1991, "Dynamic Load Capabilities of Active Electromagnetic Bearings," *ASME Trans. Journal of Tribology*, Vol. 113, pp. 598~603.

Jeon, S., Ahn, H. and Han, D., 2002, "Model Validation and Controller Design for Vibration Suppression of Flexible Rotor Using AMB," *KSME International Journal*, Vol. 16 No. 12, pp. 1583-1593.

Keith, F. J., Williams, R. D. and Allaire, P. E., 1990, "Digital Control of Magnetic Bearings Supporting a Multimass Flexible Rotor," *STLE Tribology Transactions*, Vol. 33, pp. 307~314.

Lee, C. and Kim, J., 1992, "Modal Testing and Suboptimal Vibration Control of Flexible Rotor Bearing System by Using a Magnetic Bearing," *ASME Trans. Journal of Dynamic System, Meaurement, and Control*, Vol. 114, pp. 244~252.

Lyons, J. P., Preston, M. A., Gurumoorthy, R. and Szczesny, P. M., 1994, "Design and Control of a Fault-Tolerant Active Magnetic Bearing System for Aircraft Engine," *Proceedings of the Fourth International Symposium on Magnetic Bearings*, ETH Zurich, pp. 449~454.

Maslen, E. H. and Meeker, D. C., 1995, "Fault Tolerance of Magnetic Bearings by Generalized Bias Current Linearization," *IEEE Trans. Magnetics*, Vol. 31, pp. 2304~2314.

Maslen, E. H., Sortore, C. K., Gillies, G. T., Williams, R. D., Fedigan, S. J. and Aimone, R. J., 1999, "Fault Tolerant Magnetic Bearings," *ASME Trans. Journal of Engineering for Gas Turbines and Power*, Vol. 121, pp. 504~508.

Matsumura, F. and Yoshimoto, T., 1986, "System Modeling and Control of a Horizontal-Shaft Magnetic-Bearing System," *IEEE Trans. Magne-*

tics, Vol. 22, pp. 197~206.

Meeker, D. C., 1996 "Optimal Solutions to the Inverse Problem in Quadratic Magnetic Actuators," *Ph. D. Dissertation, Mechanical Engineering*, University of Virginia.

Na, U. J. and Palazzolo, A. B., 2000, "Fault-Tolerance of Magnetic Bearings with Material Path Reluctances and Fringing Factors," *IEEE Trans. Magnetics*, Vol. 36, No. 6, pp. 3939~3946.

Na, U. J. and Palazzolo, A. B., 2001, "The Fault-Tolerant Control of Magnetic Bearings With Reduced Controller Outputs," *ASME Trans. Journal of Dynamic Systems, Measurement, and Control*, Vol. 123, pp. 219~224.

Salm, J. and Schweitzer, G., 1984, "Modeling and Control of a Flexible Rotor with Magnetic Bearing," *Proceedings of the Third International Conference on Vibrations in Rotating Machinery*, pp. 553~561.